Geofísica Internacional (2014) 53-4: 425-434

Original paper

Special 3D electric resistivity tomography (ERT) array applied to detect buried fractures on urban areas: San Antonio Tecómitl, Milpa Alta, México

René E. Chávez*, Gerardo Cifuentes-Nava, Andrés Tejero, J. Esteban Hernández-Quintero, and Diana Vargas

Received: June 21, 2013; accepted: May 20, 2014; published on line: October 01, 2014

Resumen

Las técnicas geofísicas se pueden emplear para entender las características físicas del subsuelo en áreas densamente pobladas, donde los asentamientos urbanos presentan problemas estructurales. Un ejemplo interesante se presenta en esta investigación, donde se aplica en tres dimensiones el método de Tomografía de Resistividad Eléctrica (TRE-3D) empleando arreglos alternativos que permiten investigar el subsuelo bajo las construcciones afectadas.
Se estudia un pequeño barrio compuesto por un bloque de casas dentro del pueblo de San Antonio Tecomitl. El área se encuentra hacia la planicie de la Sierra del Chichinautzin, en el límite sur de la Cuenca de México. Este asentamiento sufre de fuertes daños estructurales debido a fracturamientos y hundimientos en el subsuelo. El método TRE-3D se realizó para caracterizar el subsuelo bajo este complejo urbano. Se utilizó un arreglo de resistividad especial (geometría de ‹*herradura*‘) empleando una combinación de arreglos en "*L*", los métodos ecuatorial -dipolo y de Mínimo de Acoplamiento para ‹ *iluminar* ` en su totalidad el subsuelo que se encuentra debajo de la manzana de casas. Los modelos de resistividad calculados presentan un patrón de valores de alta resistividad, que coincide con las viviendas afectadas. Tal rasgo parece extenderse más allá de los límites de la región estudiada, y es probablemente parte de un sistema de fracturas más complejas. Es muy probable que las fracturas se produjeron debido al suelo pobremente consolidado, el cual es parte de una zona de transición; la intensa extracción de agua, que forman vacíos en el subsuelo provocando subsidencia y, finalmente, la existencia de fallas regionales de mayor extensión y profundidad que podrían controlar estas estructuras superficiales.

Palabras clave: tomografía de resistividad eléctrica 3-D, Geofísica urbana, fracturamientos, hundimientos.

Abstract

Geophysical techniques can be employed to understand the physical characteristics of the subsurface in highly populated areas, where urban settlements present structural problems. An interesting example is presented in this investigation, where three-dimensional Electric Resistivity Tomography (ERT-3D) is applied employing alternative arrays that allow investigating the subsoil beneath the affected constructions.
A small neighborhood comprised by a block of houses within the town of San Antonio Tecómitl is studied. The area is found towards the outskirts of the Chichinautzin range, in the southern limit of the Mexican Basin. This settlement suffers of strong damage in their structures due to fractures and subsidence within the subsoil. ERT-3D was carried out to characterize the subsoil beneath this urban complex. A special resistivity array (‘*horse-shoe*’ geometry) employing a combination of ‘*L*’, *equatorial-dipole* and *minimum-coupling* methods was carried out to fully ‘*illuminate*’ the subsoil beneath the block of houses. Computed resistivity models depicted a high resistivity pattern that coincides with the affected houses. Such pattern seems to extend beyond the limits of the surveyed areas, and is probably part of a more complex fracture system. It is very likely that fractures have been produced due to the poorly consolidated soil, which is part of a transition zone; the intense water extraction, that form ‘voids’ in the subsoil causing subsidence effects and finally the existence of regional faults to greater extent that might control these shallow features.

Keywords: electric resistivity tomography 3-D, urban Geophysics, fractures, subsidence.

R. E. Chávez*
G. Cifuentes-Nava
J. E. Hernández-Quintero
D. Vargas

Instituto de Geofísica
Universidad Nacional Autónoma de México
Del. Coyoacán, 04510
México D.F., México

Andrés Tejero
División de Ciencias de la Tierra
Facultad de Ingeniería
Universidad Nacional Autónoma de México
Del. Coyoacán, 04510
México D.F., México

Introduction

Urban development in modern cities requires of a more integral knowledge of the subsurface, mainly on those areas, where human concentrations increase. Mexico City is one example, where this megacity constitutes one of the largest concentrations of human activities in the world. Most of the urban area is underlain by lacustrine sediments of the former lakes, and confined by important volcanic ranges. Such sediments offer poor foundation conditions for constructive purposes. Therefore, high risk areas have to be identified to prevent accidents and disastrous events.

In the last three decades ERT-3D techniques have been developed, like the Roll-Along method to acquire 3D data (Dahlin and Bernstone, 1997). Such methodology consists on setting parallel lines that cover the study area. Observations are made in the 'x' and 'y' directions, which commonly employ the Pole-Pole array. An important amount of data can be obtained by using this technique, however data processing is cumbersome and sometimes data inversion takes too much time.

Loke and Barker (1996) designed a processing approach to decrease the number of data maintaining resolution and quality of the modeled data. This technique was named 'cross-diagonal survey', where the potential (V) observations are made in the electrodes lying in the horizontal, vertical and diagonal transects crossing the current electrode. The amount of data is reduced to the half, keeping significant quality and resolution. Aizebeokhai, *et al*. (2009) recommends a maximum separation between profiles of 4*a* in designing the survey grids, being *a* the electrode separation. Such rule guaranties good quality and resolution of the 3D resistive image of the subsoil. These techniques are suitable to open areas, as the example provided by Dahlin *et al.* (2002), when investigating karstic zones.

However, cities and in general urbanized zones present a different challenge. In this case, the urban spots extend towards the already scarce open spaces, leaving the streets to carry out geophysical observations in terms of 2D profiles. Therefore, the already mentioned 3D techniques cannot be applied. However, geophysical transects are not ideal to obtain a complete cover of the studied area (Deceuster and Kaufmann, 2003). On the other hand, the distance between parallel streets can be larger than the distance recommended by Aizebeokhai, *et al.* (2009), if grids or Quasi-3D methods are considered. Thus, interpretation of such sets of data cannot be reliable. Geophysical prospecting methods are challenged, when applied on highly urbanized areas, where habitation complexes (Trogu *et al*., 2011; Chávez *et al*., 2014), schools, historical monuments (Chávez *et al*., 2010; Argote *et al.*, 2013), prevent the positioning of profiles in parallel to form grids. In order to overcome this problem, an alternative technique is employed, that allows acquiring reliable distribution of resistivity data at depth beneath the affected area without the need of parallel transects across the constructions

An example of one of such heavily urbanized sectors within the Mexican Basin is found in Tecomitl, a small town belonging to Milpa Alta County, towards the southeastern limits of the Country's capital, which is part of the so called transition zone (Marzal and Massari, 1969). This is a small neighborhood possessing a high concentration of low- to middle-class houses comprised by one- and two-story edifications, where some of these dwellings are being affected by cracks and fissures in their constructions. County authorities are worried about the possibility of a soil collapse in this area and its disastrous effects on this community. Therefore a three dimensional Electric Resistivity Tomography (ERT-3D) was carried out to characterize the subsoil beneath the buildings, as a project to allow the authorities to establish a plan to remediate the vulnerable zones.

ERT-3D Methodology

Unfortunately, there is no sufficient space to deploy the geophysical transects through the dwellings and settlements composing this locality due to the heavy urbanization this neighborhood possesses. Therefore, a special array type (*Horse-Shoe* geometry) was employed (Argote *et al.*, 2013; Tejero *et al.,* 2014). The so named *horse-shoe* array employed in this investigation is a combination of different special arrays designed to cover the subsurface by means of a series of apparent resistivity observations at depth. These arrays are the '*L*-array' (Chávez *et al*., 2011; Tejero *et al.,* 2014), the equatorial (*EQ*) and the minimum coupling (*MC*) settings (Argote *et al.*, 2013).

This special geometry attempts to cover the subsurface with resistivity observations underneath the neighborhood. ERT-3D data was acquired employing a Syscal-Pro resistivimeter (IRIS Instruments) with 48 channels. Electrodes were inserted deep enough (~0.6 m) to make contact with the '*natural*' soil, with a separation of 4m. Cables and electrodes were

deployed along the narrow streets surrounding the neighborhood studied. The *horse-shoe* dispositive designed to survey the area possesses a length on each side of 80 m long, approximately. Display of apparent resistivities at depth were computed with the help of the software Electre-Pro (Iris Instruments, 2010), which computes the attribution point of each apparent resistivity measured at depth

The *L*-array

This ERT array was explained in detail by Chávez *et al.* (2011) and Argote *et al.* (2013). In this case, two perpendicular ERT profiles are needed. The horseshoe arrangement employed in this investigation is depicted in Figure 1. This array allows surrounding the structure to be studied. In this particular example three 'L's are carried out. The WS array is employed; the current electrodes (in red) are moved one electrode as well as the potential electrodes (Figure 1A), where the arrows define the direction of movement. Figure 1B depicts the distribution at depth of the apparent resistivities measured. Separation between current electrodes is increased by two electrode positions and the procedure is repeated once more. The process ends when the all electrodes in this geometry are used.

Dipole-Equatorial (*EQ*) array.

Such an array needs two parallel ERT lines (Figure 2A), where the current electrodes are kept fixed at the corner of each ERT line. The potential electrodes (M, N) will move in the direction of arrows until the total number of electrodes in each line is completed. Then, the current electrodes (A, B) move one electrode up (A). The resulting subsurface resistivity observations are displayed in (Figure 2B). It is possible to observe that each point at depth as well as the shallow line of observations is generated for each electrode change along the parallel transects (P1 and P2).

Minimum Coupling (*MC*) array.

Two parallel lines are also needed to carry out the apparent resistivity observations, as mentioned above. The current electrodes are set at the corners of each ERT. In this array (Figure 3A), the current electrodes are fixed (A, B), whereas the potential (M, N) electrodes move along the P1-P1' line in the S-N direction. Such process continues until the last electrode is reached. Then, the current electrodes move one electrode space up and the process start again. The progression is over when the last electrode is reached. Then, the same procedure follows with the next line (P2-P2') and everything goes exactly the same. Observe the apparent resistivity distribution at depth obtained with this process. Two different resistivity patterns are obtained.

Area Of Study

The area under study is found towards the southern portion of the Basin of Mexico, within the San Antonio Tecómitl town (Figure 4A). Geologically speaking, the area belongs to a transition zone identified by Marsal and Mazzari (1969). These authors divided the Basin of Mexico in three different regions. Zone I (Hilly zone) is formed by harder materials products of past eruptive events and found in the high

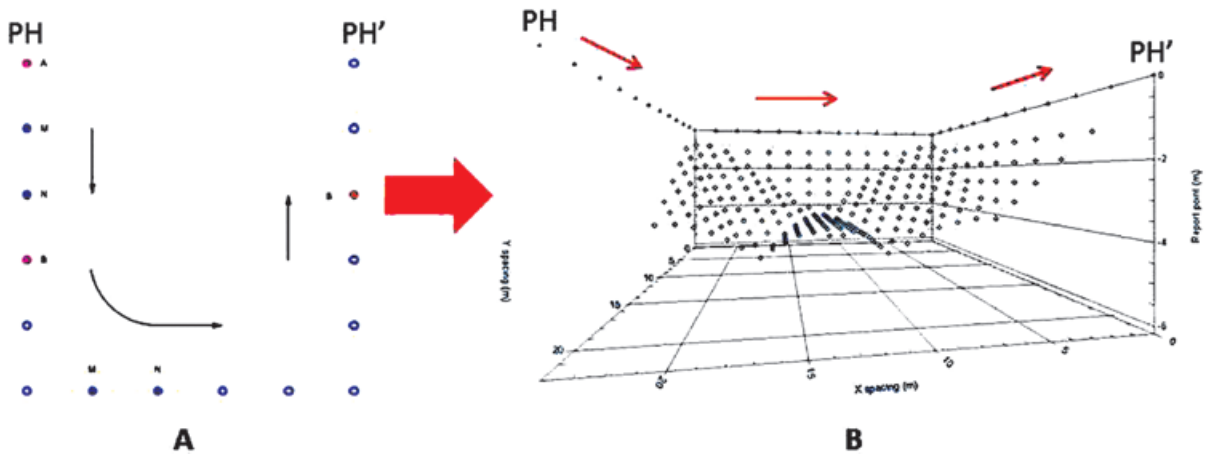

Figure 1. Sequence designed to calculate the '*L*' array (A), A and B indicate the current electrodes and M and N the potential electrodes. The computed distribution of observed apparent resistivities as measured by the resistivimeter is shown (B).

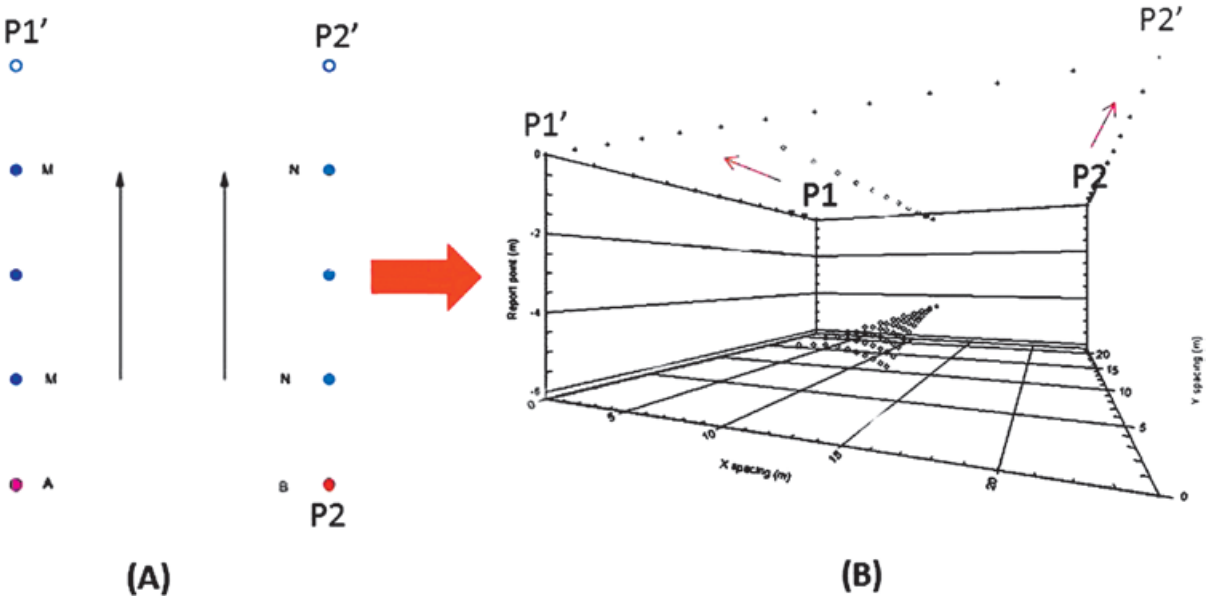

Figure 2. Sequence designed for the Equatorial Dipole dispositive (A) and the distribution of measured apparent resistivities at depth (B) are depicted.

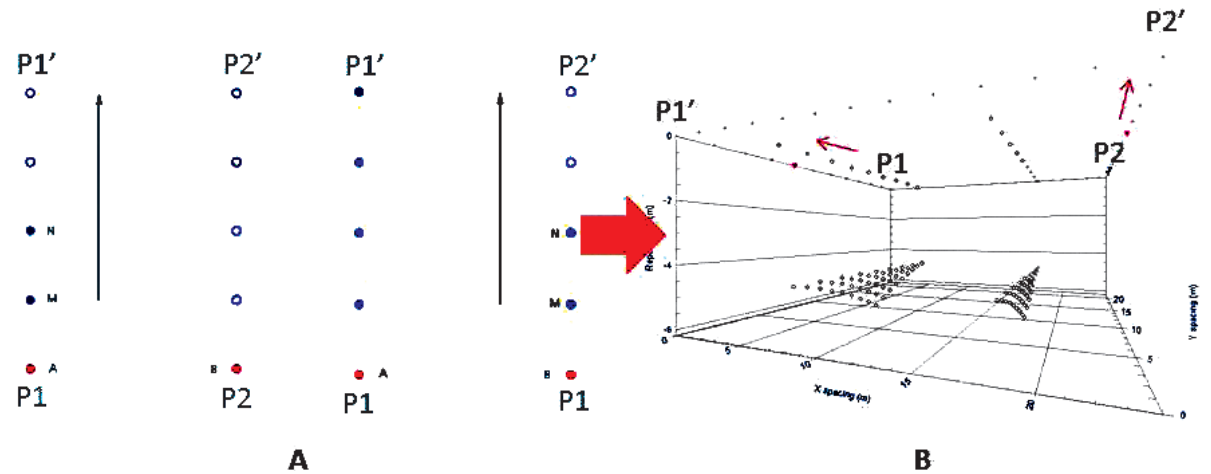

Figure 3. Sequence designed for the Minimum Coupling (MC) (A) and distribution at depth of apparent resistivities (B) are displayed.

ranges surrounding the basin. They have good load capacity and negligible compressibility. Zone II is a region that possesses poor stability, suffering of differential subsidence effects. Finally, Zone III ((Lacustrine Zone) is composed mainly by clayey sediments, and poorly consolidated materials that once were the bottom of the ancient lake of Texcoco in pre-Hispanic times. This small urbanized region is found on top of clays and sand lenses interbedded with soft eruptive materials (volcanic tuffs).

Some of the dwellings composing the studied area present important damages in their foundations, walls and roofs. Images depicted by Figures 4B and 4C show part of the damage found in the constructions located in this neighborhood. Subsidence effects and fractures observed in many portions of the dwellings are possibly produced by the ground water extraction; rain water flows from the highlands that undermine the shallow sedimentary layers at depth, and possible problems of anthropogenic origin, like water leaks from the water distribution network and so on.

ERT-3D Investigation

The geophysical study was carried out within the boundaries of a block of houses to characterize the subsoil beneath this settlement. Figure 5A outlines the horse-shoe array. Each circle and number depicts the position of every electrode along the streets surrounding the neighborhood. The main goal is to detect a fracture that crosses underneath, where evidence of such a feature can be observed in several homes, in terms of fissures in walls, and small fractures on the paved roads.

Figure 5B depicts the observations at depth as calculated by using the program ElectrePro (IRIS, 2010). A total of 824 resistivity observations at depth can be estimated, depicted as black dots. A good coverage towards the northern portion of the working cube is attained. Black squares in the image depict the location of the 48 electrodes deployed partially surrounding the neighborhood. Unfortunately, the southern portion of the measured square could not be closed, due to the heavy traffic found in 5 de Mayo Avenue. We could not get permission by the local authorities to close the traffic in that street.

It is possible to observe the measured apparent resistivities calculated by the program Electre-Pro and visualized with a special representation program. Figure 6 displays the 824 apparent resistivities at depth. Each color determines the resistivity value measured with the resistivimeter, note that negative values are present. Such type of data is due to the methodology employed to compute every data point at depth. Yellow circles define the position of the electrodes. The highest variation in these values is found towards the northwestern portion of the *horseshoe* array, where low (~10 Ohm-m) to high (>200 Ohm-m) apparent resistivity values have been measured. In general, apparent resistivity values are around 100 Ohm-m, which suggests that this is the average resistive value for the subsoil. Even if high resistive values are found in the deepest line provided by the MC array, it is clear that resolution at that depth with the array employed will be poor. Therefore, the array presented in this investigation may resolve anomalous resistivities located up to a depth of 20 m, approximately. Deeper resistive structures will have no meaning, and then a constraint can be added to the inversion process in terms of the maximum depth to be investigated.

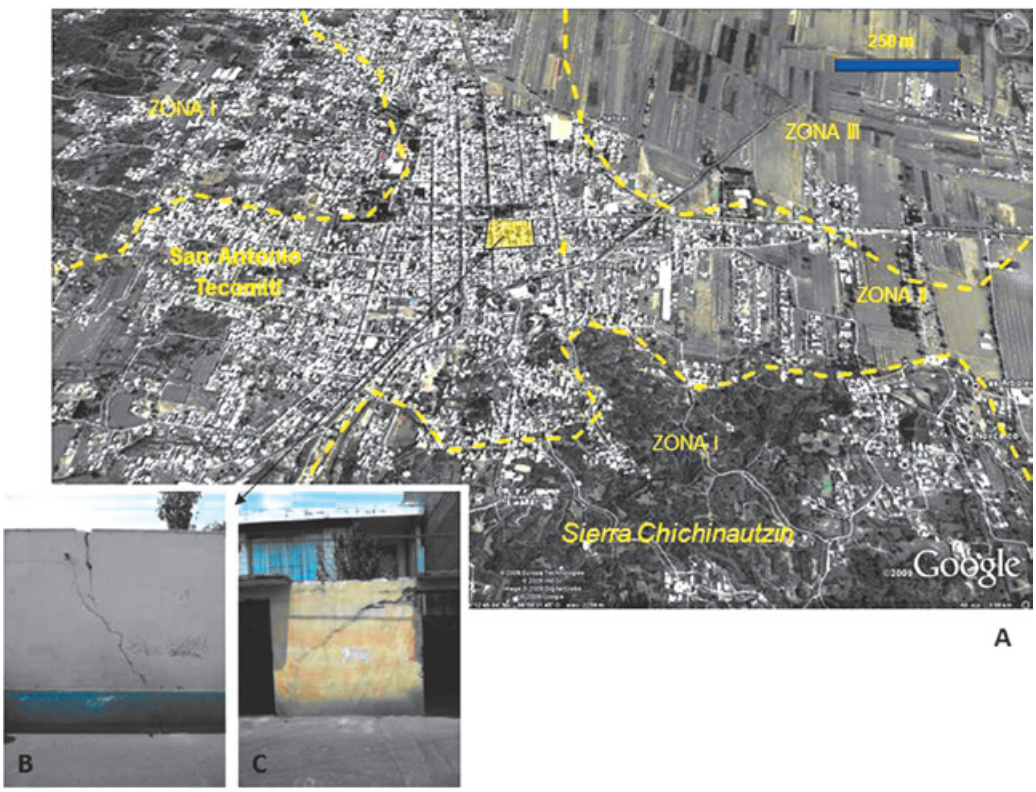

Figure 4. The satellite image (Google, 2012) displays the San Antonio Tecomitl town. The inset depicts the different damages (B) and (C) observed in the study area. Note fissures and cracks on walls.

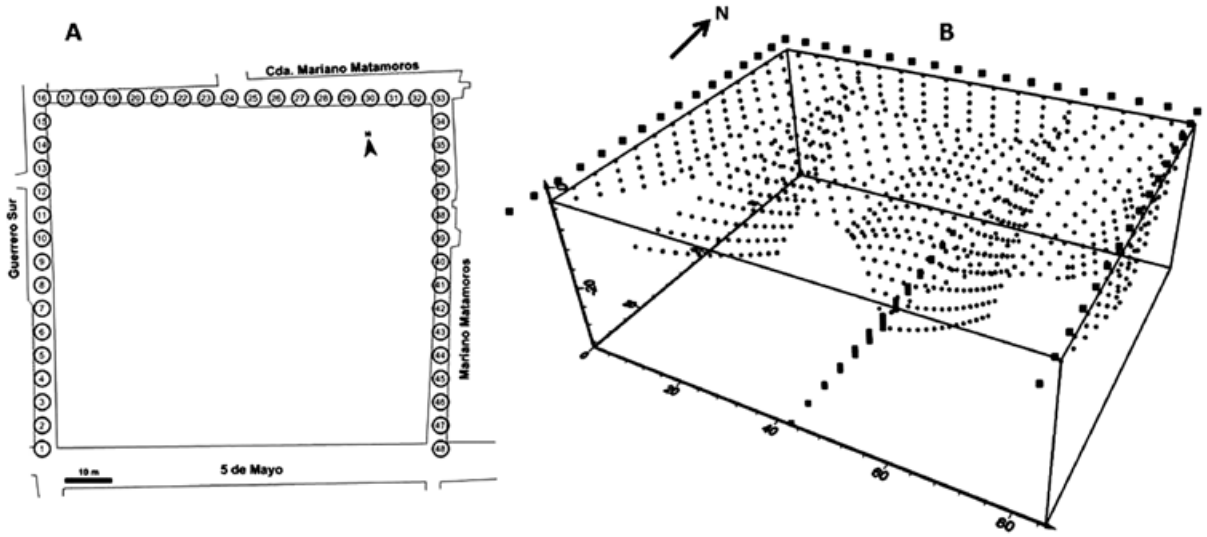

Figure 5. The *horse-shoe* array designed to study the affected block of houses. Circles and numbers indicate the location of the electrodes (A). The computed distribution of apparent resistivities at depth is depicted (B). 824 quadripoles are computed with a maximum penetration depth of 20 m.

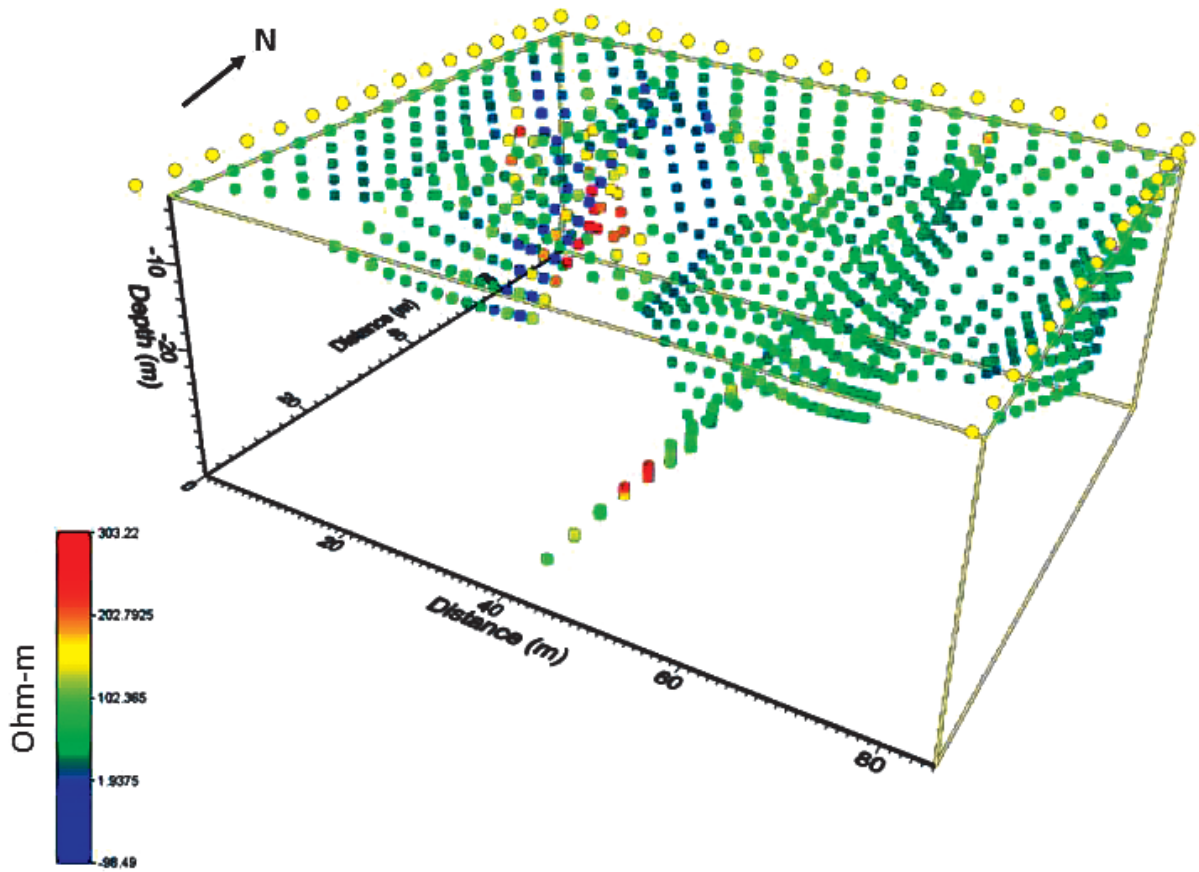

Figure 6. Measured resistivities at depth obtained from the field survey. Colors indicate the observed apparent resistivity value.

The inversion process carried out to compute the three dimensional resistivity model is an important module of the EarthImager3D (AGI, 2012) commercial package. This is based on the methodology described by Loke and Barker (1996), which is explained in detail by Tejero *et al.* (2002). The mathematical modelling of the real resistivities at depth includes several steps to arrive to a final solution. Initially, a starting model is constructed based on a given apparent resistivity distribution at depth. In this case, a half-space with a constant resistivity is assumed. Then, a selection of a non-linear optimization technique can be performed. Such a procedure must include the solution of a linearized inverse problem based on the current model and data misfit for a model update. Therefore, the elements of a Jacobean matrix must be assessed to finally solving the system of equations. It is important to mention that the underdetermined and ill-posed nature of the 3D resistivity data, which generally speaking, most of the geophysical data share; makes the inverse solution non-unique and ambiguous. Therefore, additional constraints or other type of criteria must be imposed to obtain a reasonable solution. In this investigation, we have employed the smooth model inversion, which is also known as Occam's inversion (Lines and Treitel, 1988; DeGroot-Hedlin and Constable, 1990). This type of process assumes that errors follow a Gaussian distribution (Tejero *et al.*, 2002).

The misfit between the observed and computed values can be represented as the dispersion of the computed resistivity values in terms of the observed apparent resistivities. Figure 7A depicts the cross-plot calculated by the commercial program employed (EarthImager3D), which allowed to keep track of every inverted step. An initial RMS value of 20% is obtained for the first iteration process, where 8 iterations followed to reach a final solution. The corresponding cross-plot shows a much better fit between the observed and computed data (Figure 7B), with the corresponding RMS error computed of 8.9%.

The inverted solution shows a high resistive alignment, which could be associated to a possible fracture (Figure 8A). As expected, the southern portion of the resistivity cube lacks of resolution. Figure 7B depicts the working cube from the top, and Figure 7C from the bottom, selecting a high resistivity (160 Ohm-m to 1,000 Ohm-m) interval. It is clear the high resistivity values depicting a NE-SW feature. Such an alignment can be associated to the presence of a fracture.

These high resistive values (~1000 Ohm-m) can be explained by assuming that the low consolidated materials forming this lacustrine basin (mainly clays) may fill the fracture, increasing its apparent resistivity, which is proportional to their porosity. It is expected that pores within the clays are mostly occupied by air, which behaves as a dielectric fluid, during the dry season (Ovando-Shelley *et al*., 2007).

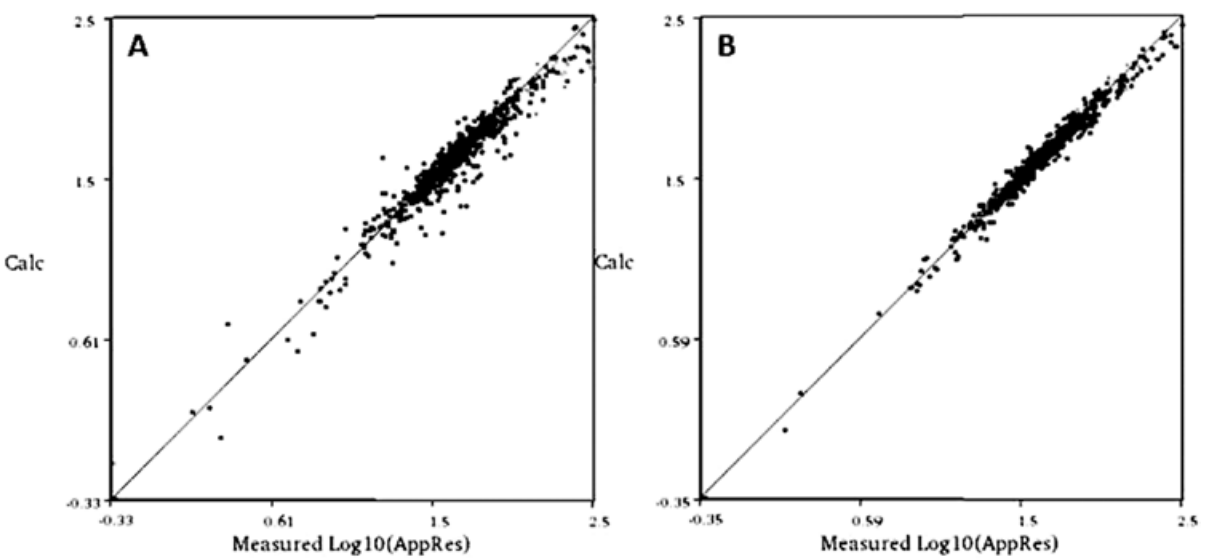

Figure 7. Apparent resistivity cross-plots calculated for the initial iteration (A) and the final iteration (B). 8 iterations were needed to come up to a final inverted resistivity model.

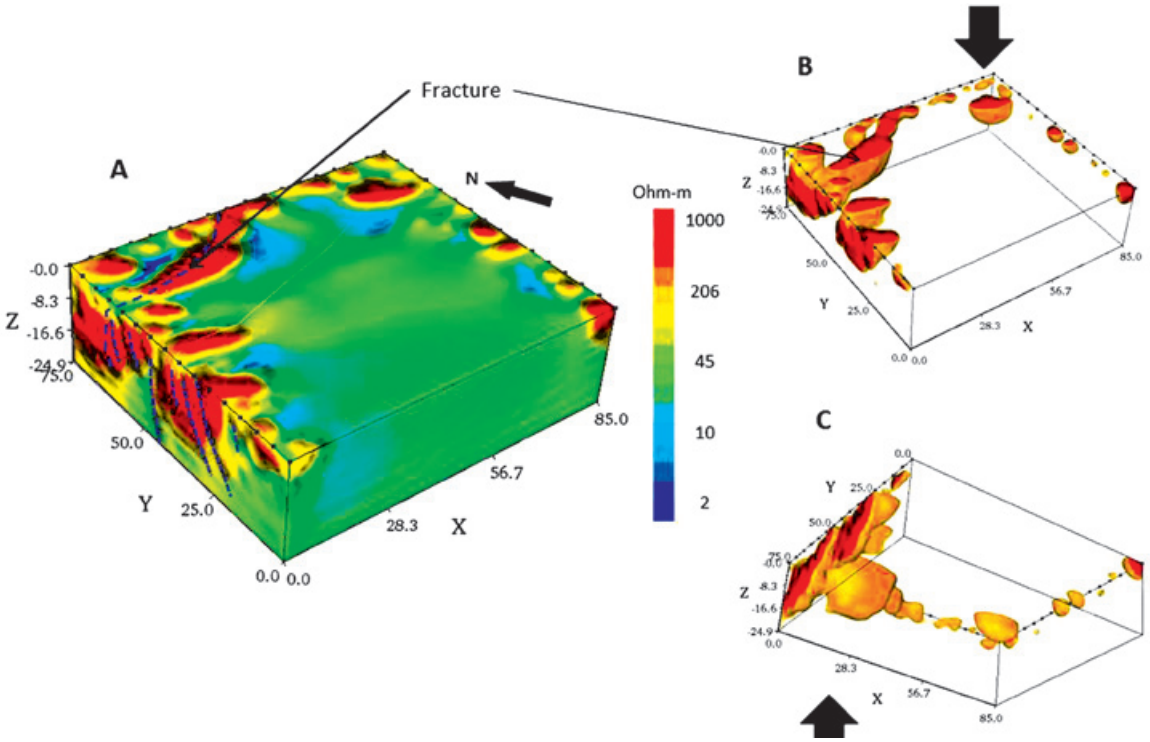

Figure 8. The inverted cube is shown (A). High resistivity values can be associated to a fracture. Images to the right depict the working cube from the top (B) and from the bottom (C). Only high resistive values (~1000 ohm-m) are depicted to observe clearly the resistive anomaly.

Figure 9. The working cube is observed from the top. The Google image (Google, 2012) is superimposed on top of the resitivity anomalies. Observe the fracture in the NE-SW direction.

The 3D model has been superimposed over the satellite image (Google-Earth, 2012) in Figure 8. It is possible to observe that the high resistive alignment crosses in the NE-SW direction a series of houses within the studied neighborhood. Some of the fissures and cracks observed on the pavement and walls of houses coincide with the detected structure (Figure 4B and Figure 4C). These problems in the subsoil can be attributed to differences in water content leading to subsidence problems beneath houses or a differential compaction of sands and clays comprising the materials forming the Zone II.

Conclusions

The 3D methodology employed with the '*horse-shoe*' array discussed in this investigation resolves adequately the characteristics of the subsurface. This methodology loose shallow information, due to the missing data points at the central and southern portions of the array, where no-electrodic line could be set, nevertheless, reliable information up to a depth of 20 m can be attained.

Computed resistivity models depicted the buried fracture pattern affecting the urban complexes. Such pattern seems to extend beyond the limits of the surveyed areas, and is probably part of a more complex fracture system. It is very likely that fractures have been produced due to the poorly consolidated soil, which is part of a transition zone (Zone II, according to Marssal and Massari, 1969); the intense water extraction, that form 'voids' in the subsoil causing subsidence effects and finally the existence of regional faults to greater extent that might control these shallow features.

Results provided useful information about the resistivity distribution beneath the areas studied, leaving to the corresponding authorities to define the remediation process to be carried out in this section of San Antonio Tecomitl to avoid possible collapses of the subsoil.

This methodology provides of a new alternative tool to investigate the subsurface beneath constructions, where it is not possible to set a traditional ERT-3D array in urban populated areas or buildings.

Aknowledgments

We thank the authorities of the Milpa Alta County, Dirección de Protección Civil for allowing us to carry out the field survey within the San Antonio Tecomitl urban zone. We are also grateful to the Engineering Geophysics students from the Faculty of Engineering UNAM for helping us in the field work. This study was financed by the Mexico City's Secretaría de Ciencia, Tecnología e Inovación agreement # PINV11-6. D. Vargas received a scholarship from this project.

References

AGI, 2010, EarthImagerTM 2D and 3D, Resistivity and IP inversion software: Advanced Geosciences Incorporated, www.agiusa.com.

Aizebeokhai A.P., Olayinka A.I., Singh V.S., 2009, Numerical evaluation of 3D geoelectrical resistivity imaging for environmental and engineering investigations using orthogonal profiles, SEG *Expanded Abstracts*, 1440, doi:10.1190/1.3255120.

Argote-Espino D., Tejero-Andrade A., Cifuentes-Nava G., Iriarte L., Farías S., Chávez RE., López F. 2013. 3D electrical prospection in the archaeological site El Pahñu, Hidalgo State, Central Mexico: *Journal of Archaeological Science*, 40, 1213-1223.

Chávez G., Tejero A., Alcantara M.A., Chavez R.E., 2011. The 'L-Array', a tool to characterize a fracture pattern in an urban zone: Extended Abstracts of the 2011 Near Surface Geophysics meeting, *European Section Meeting* (Printed in CD), Leicester, UK.

Chávez R.E., Tejero A., Cifuentes G., Hernández E., Aguilar D., 2014, Imaging fractures beneath a residential complex using novel 3D electrical resistivity arrays: *Journal of Environmental and Engineering Geophysics*. In revision.

Dahlin T., Bernstone C., 1997, A roll-along technique for 3D resistivity data acquisition with multi-electrode arrays: 10th *Annual Meeting of the Symposium on the Application of Geophysics to Engineering and Enviromental Problems*, 927-35.

Dahlin T., Bernstone C., Loke M.H., 2002, A 3-D resistivity investigation of a contaminated site at Leernaken, Sweden, *Geophysics*, 67, 1692-1700.

Deceuster J., Kaufmann O., 2003, Applications des tomographies en résistivité électrique 3D à la reconnaissance de zones Karstifiées, Belgique, *Actes du 4ème Colloque GEOFCAN*, 143-150.

DeGroot-Hedlin D., Constable S., 1990, Occam's inversion to generate smooth, two-dimensional models from magnetotelluric data, *Geophysics*, 55, 1613-1624.

Google-Earth, 2012, www.google.com.mx/intl/es/earth/.

IRIS, 2010, ElectrePro@ software: User manual. www.iris-instruments.com.

Lines R.L., Treitel S., 1988, Tutorial: A review of least-squares inversion and its application to geophysical problems, *Geophysical Prospecting*, 32, 159-186.

Loke M.H., Barker R.D., 1996, Practical techniques for 3D resistivity surveys and data inversion. *Geophysical Prospecting*, 44, 449-523.

Tejero A., Chávez R.E., Urbieta J., Flores-Márquez E.L., 2002, Cavity detection in the south-western hilly portion of Mexico City by resistivity imaging: *Journal of Engineering and Environmental Geophysics*, 7-3, 130-139.

Tejero A., Cifuentes G., Chávez R.E., López-González A., Delgado-Solorzano C., 2014, "L" and "Corner" arrays for 3D electrical resistivity tomography: An alternative for urban zones: *Near Surface Geophysics*. In press.

Trogu A., Ranieri G., Fischanger F., 2011, 3D electrical resistivity tomography to improve the knowledge of the subsoil below existing buildings: *Environmental Semeiotics*, 4-4, 63-70.